Review of Scientific Instruments

High frame rate emission spectroscopy for ablation tests in plasma wind tunnel

Cite as: Rev. Sci. Instrum. **92**, 033101 (2021); https://doi.org/10.1063/5.0040801
Submitted: 16 December 2020 • Accepted: 04 February 2021 • Published Online: 01 March 2021

Ranjith Ravichandran, David Leiser, Fabian Zander, et al.

Review of Scientific Instruments ARTICLE scitation.org/journal/rsi

High frame rate emission spectroscopy for ablation tests in plasma wind tunnel

Cite as: Rev. Sci. Instrum. 92, 033101 (2021); doi: 10.1063/5.0040801
Submitted: 16 December 2020 • Accepted: 4 February 2021 •
Published Online: 1 March 2021

Ranjith Ravichandran,[1,a)] David Leiser,[1] Fabian Zander,[2] Stefan Löhle,[1] Pavol Matlovič,[3] Juraj Tóth,[3] and Ludovic Ferrière[4]

AFFILIATIONS

[1]High Enthalpy Flow Diagnostics Group, Institute of Space Systems, University of Stuttgart, 70569 Pfaffenwaldring, Stuttgart, Germany
[2]Institute for Advanced Engineering and Space Sciences, University of Southern Queensland, Toowoomba 4350, Queensland, Australia
[3]Faculty of Mathematics, Physics and Informatics, Comenius University in Bratislava, Mlynska Dolina, 842 48 Bratislava, Slovakia
[4]Natural History Museum, Burgring 7, 1010 Vienna, Austria

[a)]**Author to whom correspondence should be addressed:** rravichandran@irs.uni-stuttgart.de

ABSTRACT

This article describes a novel high frame rate emission spectroscopy setup developed for measurements in high enthalpy flow fields. The optical setup and the associated hardware arrangements are described in detail followed by test case data to demonstrate the capability of recording spectral images at 1 kHz frame rate. The new system is based on a classical Czerny–Turner spectrograph but with a particular setup for high frame rate detection using a Generation II intensifier coupled with a high-speed camera. The high frame rate spectral images acquired enable, for the first time, investigation of the spatial distribution and temporal tracking and evolution of molten droplets of an ablating sample. In this paper, an example is shown from ablating meteorite samples tested in a high enthalpy plasma flow field corresponding to a flight scenario at an altitude of 80 km. This new instrumental configuration allows emission spectroscopic analysis of transient phenomena simulated in the high enthalpy ground test facilities with kHz resolution. The particular feature of this system is the ability to measure very faint spectral lines at high temporal and spatial resolution.

I. INTRODUCTION

Emission spectroscopy, the diagnostic method based on the investigation of light emitted from a medium of interest by analyzing the wavelength distributed intensities, is a fundamental tool for non-intrusive diagnostics. Particularly in low density but high enthalpy flow fields, for example, experienced during atmospheric entry flights, this diagnostic method allows an excellent analysis of the chemical state of the gas flow.[1–3] To date, wavelength-resolved emission spectroscopy was applied mostly as a single image technique. Temporal and/or local resolution using a number of frames during a short time interval become necessary for transient and high-speed phenomena. This paper shows a new setup that uses a high frame rate imaging camera with a Czerny–Turner spectrometer, which allows us to investigate spectral and local phenomena on a millisecond time scale.

Emission spectroscopic measurements made in high enthalpy ground test facilities typically employ an intensified charge coupled device (ICCD) to acquire a spectral image by recording the diffracted light coming out of the spectrometer. Generally, these ICCDs are capable of recording images at a frame rate of only a couple of Hz. In impulse facilities, this results in only one image per experiment.[4] Multiple images could be obtained if the facility and the studied phenomena are relatively long duration ones. The most recent advancement in the commercial ICCDs provides dual image modes in microsecond intervals or the ability to use higher frame rates by binning modes, as demonstrated by Zander *et al.*[5] However, these methods are not sufficient to temporally resolve the spectral data for

spatially varying and relatively high-speed phenomena such as the ablation of meteorites and spacecraft thermal protection materials, which are commonly tested in plasma wind tunnel facilities. Fragmentation is another transient phenomenon of interest during meteoroid entry.[6] Even though the plasma facilities can be operated for relatively long duration, ablation phenomena involve a lot of important features occurring, and spalled/ablated products evolving, in a very short time scale. In order to capture the millisecond-scale processes in the spectral domain, emission spectroscopy applied at high frame rates becomes necessary. This is realized in this experimental work by using a high-speed camera coupled with an intensifier at the exit of a Czerny–Turner spectrometer to record emission spectra of ablating meteorites at frame rates in the order of kHz.

Meteorite ablation tests and the test conditions in plasma wind tunnels are discussed in Sec. II. The details of the instrument configuration are explained in Sec. III followed by the calibration procedure in Sec. IV. The successful application of this instrument is demonstrated in Sec. V with the high-speed spectral data obtained for the ablation of a meteorite.

II. METEORITE ABLATION IN PLASMA WIND TUNNELS

The new technique developed is required to study the fast transient process of an ablating meteorite. In the High Enthalpy Flow Diagnostics Group (HEFDiG) of the Institute of Space Systems at the University of Stuttgart, meteoroid entry scenarios are investigated in order to provide datasets needed by observers and meteor physicists and to support the fundamental study of meteoroids. The recording of meteor spectra helps in understanding the elemental composition of meteoroids[7] and possible estimation of their trajectory and orbital parameters[8] and ultimately identifying their parent bodies such as asteroids and comets. Meteor spectra have been recorded by direct observation during meteor showers and by constant monitoring of the night sky, for example, using the global All-sky Meteor Orbit System (AMOS) meteor network[9] and at a few other locations across the world. Recently, meteorite samples have been exposed to representative high enthalpy atmospheric entry conditions in plasma wind tunnels and it was demonstrated as a very useful ground testing method to study the meteorite ablation by various optical diagnostics including recording its emission spectra.[10] Plasma wind tunnels have also been used to study several other problems such as testing thermal protection materials for spacecraft or re-entry object's breakup, [11–14] where the application of this high frame rate spectroscopy would be very valuable.

In this work, meteorite samples were exposed to a representative Earth-entry condition corresponding to an enthalpy of 68 MJ/kg and a stagnation point cold wall heat flux of 4.1 MW/m^2 (measured by a flat-faced 80 mm diameter probe) generated by the plasma wind tunnel facility PWK1.[15] Processes such as meteorite melting, evaporation, and ultimately the formation of a fusion crust are reproduced by testing under these plasma conditions.[10] In addition to the high frame rate emission spectroscopy, other optical diagnostics such as Echelle spectroscopy, photogrammetry, two-color ratio pyrometry, linear pyrometry, filtered thermography, videography, and light field imaging were also employed to probe the ablating meteorite. This article focuses on the new high-speed emission spectroscopy setup and presents the results from one of the meteorite test cases.

III. INSTRUMENT CONFIGURATION

The instrument configuration used for the high frame rate spectroscopy measurements in the PWK1 plasma wind tunnel facility is illustrated in Fig. 1, along with the external optical arrangement. The spectrometer used was from Princeton Instruments (Acton 2750) with a 300-grooves-per-millimeter (gpmm) grating centered at 550 nm wavelength. The high-speed camera was from Optronis Co., capable of recording at a maximum frame rate of 5 kHz at a full resolution of 512 × 512 pixels^2 and as high as 40 kHz with a reduced resolution. Spectral features such as atomic lines can be very faint, and therefore, measuring such features at high frame rates is challenging. For the new instrument in this work, an intensifier (HiCATT from Lambert Instruments) was added in front of the camera, as illustrated in Fig. 1. The system comprising an intensifier and a camera was used previously as a filtered imaging system to investigate the CO_2 plasma by Zander *et al.*[16] Recently, a similar method to the one presented here was used in the hypersonic expansion tube X3 at the University of Queensland by Andrianatos.[17]

The investigated plane of sight is a slice in the flow field along the stagnation line comprising the freestream plasma flow,

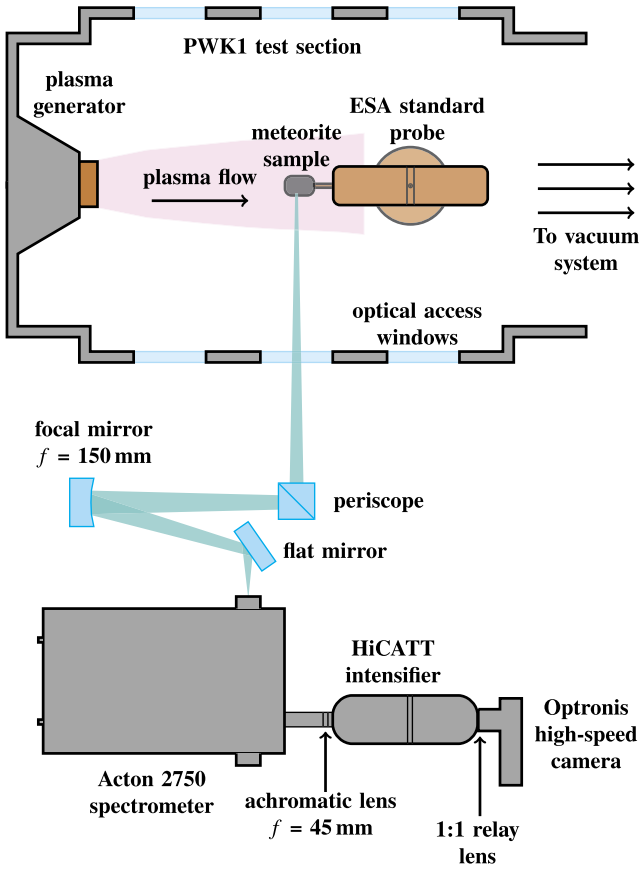

FIG. 1. Top-view schematic of the high frame rate spectroscopy optical arrangement. Illustration only, not to scale.

meteorite ablation layer, meteorite specimen, and further downstream, as illustrated in Fig. 2. This horizontal slice in the flow field was chosen for investigation as it can provide the details on the evolution of the meteorite ablation species and molten droplets as they travel downstream along the plane of sight. The external optical arrangement was used to collect the light and aim it onto the spectrometer entrance slit. It uses a periscope to rotate the light by 90° so that the horizontal plane of sight can be projected onto the vertical entrance slit of the spectrometer. A concave mirror of focal length f = 150 mm was used to form a focused image at the entrance slit. Furthermore, a flat mirror was used to deflect the light beam onto the entrance slit so that it enters the spectrometer normal to the slit. The distance from the test specimen center line to the focal mirror is d_o = 1765 mm, and accordingly, the distance from the focal mirror to the spectrometer entrance slit becomes d_i = 164 mm, following the lens equation

$$\frac{1}{f} = \frac{1}{d_o} + \frac{1}{d_i}. \tag{1}$$

The magnification M is then given by

$$M = \frac{d_i}{d_o} = 0.093. \tag{2}$$

The pixel pitch of the Optronis camera is 16 μm, resulting in a usable sensor area of 8.192 × 8.192 mm^2 for 512 × 512 pixels^2 in the camera array. The light inside the spectrometer is collimated by a mirror, diffracted by the grating, and then reflected by another mirror onto the exit port so that a focused image is again formed at the exit. The use of an intensifier in front of the camera adds more distance to the optical path, and the image was again focused by using an achromatic lens (f = 45 mm) in front of the intensifier, which altered the magnification to 0.058. The image at the camera was ultimately focused by finely adjusting the distance between the achromatic lens and the spectrometer exit. For this configuration, the distance from the image plane at the spectrometer exit to the achromatic lens is ~117 mm. The distance from the achromatic lens to the intensifier inlet is ~53 mm; however, the location of the image plane inside the intensifier system is inaccessible. As the magnification of the image coming out of the intensifier is preserved by the in-built 1:1 relay lens at the intensifier exit, the final magnification achieved at the camera is 0.058. With all the optical elements and distances and the camera detector array size, the final spatial distance captured in a spectral image corresponds to ~142 mm in the flow field and a wavelength range of 58 nm. An achromatic lens was used after the spectrometer exit to avoid any spherical and chromatic aberration, which provides a single focal plane for the light rays at different wavelengths. The optical path from the spectrometer exit to the intensifier input was enclosed with the achromatic lens housed inside a lens tube, as shown in Fig. 3.

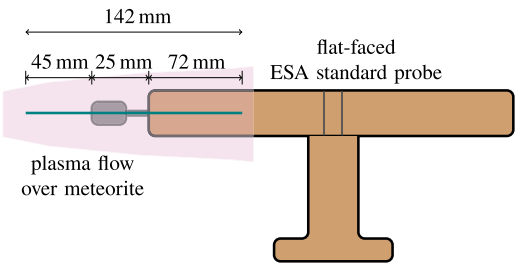

FIG. 2. Illustration of the plane of sight (green thick line) covering the freestream plasma, ablating meteorite, and flow downstream with the dimensions marked (not to scale).

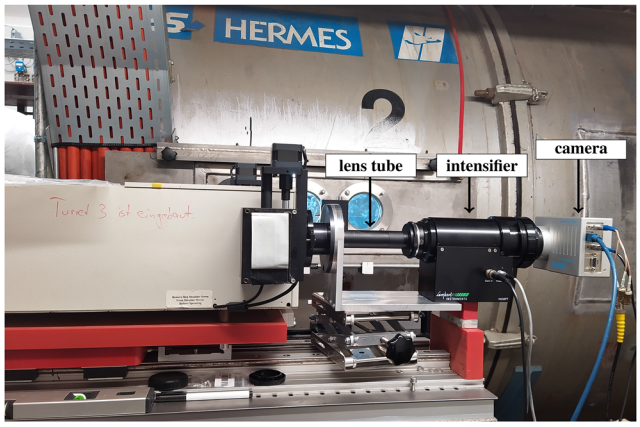

FIG. 3. Picture showing the intensifier-coupled camera arrangement with the lens tube connecting the spectrometer exit and the intensifier. The external optics before the entrance slit is not visible.

TABLE I. Wavelength dispersion and range covered for different gratings using the SpectraPro 2750 spectrometer and the intensifier/camera configuration.

	Wavelength dispersion		
Grating	Original (nm/mm)	Enhanced (nm/mm)	Range (nm)
300 gpmm	4.4	7.1	58
600 gpmm	2.1	3.4	28
1200 gpmm	1.0	1.6	13

The use of the achromatic lens after the spectrometer exit not only alters the final magnification but also enhances the wavelength dispersion accordingly. Table I shows the wavelength dispersion, both original and enhanced, for different gratings in the SpectraPro 2750 spectrometer. As the 300 gpmm grating covers the widest wavelength range possible for the given configuration, it was chosen for all the tests.

The spectral images were recorded by the high-speed camera at a frame rate of 1 kHz with the intensifier gate time of 1 ms for each frame. The recorded video data were stored as .0 data format by the camera handling software (Testbench version 2.5.30), which was then exported as individual images for post-processing using MATLAB scripts.

IV. CALIBRATION OF SPECTRAL IMAGES

An integrating sphere (ISS-5P from Gigahertz-Optik) was used to calibrate the emission intensity of the spectra recorded. The size of

the integrating sphere light output port (20 mm in diameter) combined with the magnification of the system covers only about one-tenth of the camera array at a given spatial location, and hence, the image of the integrating sphere was recorded at multiple locations along the plane of sight to cover the whole array of the camera. These images were finally joined together to obtain a full image covering the whole array. The counts from this full image, after subtracting dark current counts, were used for the flat-field calibration that provides the response of each pixel for a given known light intensity. It was then scaled with the exposure time of the actual experiments to obtain a calibrated intensity for each frame in the video. Any potential non-linearity of the intensifier response is not considered in this work and will be investigated in the future. The objective here is to demonstrate the advantages and significance of recording emission spectra at high frame rates for an ablating specimen, which delivers spatial and temporal resolution simultaneously.

V. MEASURED HIGH FRAME RATE SPECTRAL IMAGES

The ablation of meteoroids as they enter the atmosphere has been conventionally studied by meteor observations and spectral records. Here, a plasma wind tunnel capable of simulating high enthalpy atmospheric entry flows was employed to test the ablation of various meteorite specimens with their emission spectra recorded at high frame rates.

A spectral image of the ablating Knyahinya meteorite (ordinary chondrite of type L/LL5; Sample NHMV_ID_No. 13638) from the video recorded at 1 kHz is shown in Fig. 4. The horizontal axis of the spectral image corresponds to the wavelength, which has been calibrated using a UV lamp with known Hg(Ar) lines. The vertical axis represents the physical distance of the measured flow field, which has been calibrated using a metal grid of known spacing and size.

The calibrated spectral image shown in Fig. 4 corresponds to a time instance of t = 2163 ms after the probe was inserted into the center of the plasma flow. The plasma flow is from bottom to top in the image, and the spatial axis is adjusted so that the tip of the meteorite is at y = 0 mm; negative values mean upstream, and positive values mean downstream. The image captures the brighter region of the molten surface of the meteorite with two more molten droplets/vaporization spots distinctly visible downstream. At line 2, the fragment is evaporated with only spectral features visible, whereas, at line 3, the fragment is still in a molten state showing both spectral radiation and continuum radiation. From the image, the projected size of the droplets can also be determined. The wavelength distribution of spectral radiance at various spatial locations (indicated by white lines in the spectral image) was extracted and plotted in the bottom panel of Fig. 4 to compare the emission intensity of species. The data extracted from a given location (or a given pixel) are actually an average of values over three pixels in the spatial dimension, including the pixels on either side of the chosen one. A few lines have been identified with the atomic species emitting them; iron (Fe), chromium (Cr), and sodium (Na), as shown in the bottom panel of Fig. 4. The intensity of spectral features shows the spatial changes observable in a given time instance. The Na line at line 3 shows a very abrupt drop in intensity, the reason for which is unclear. This could be due to a local rise in the number density of Na atoms, resulting in self-absorption. However, it is also unclear whether this could have occurred due to the explosion of chondrules, resulting in the release of relatively more Na atoms than other elements or because of varying evaporation mechanism of various elements.

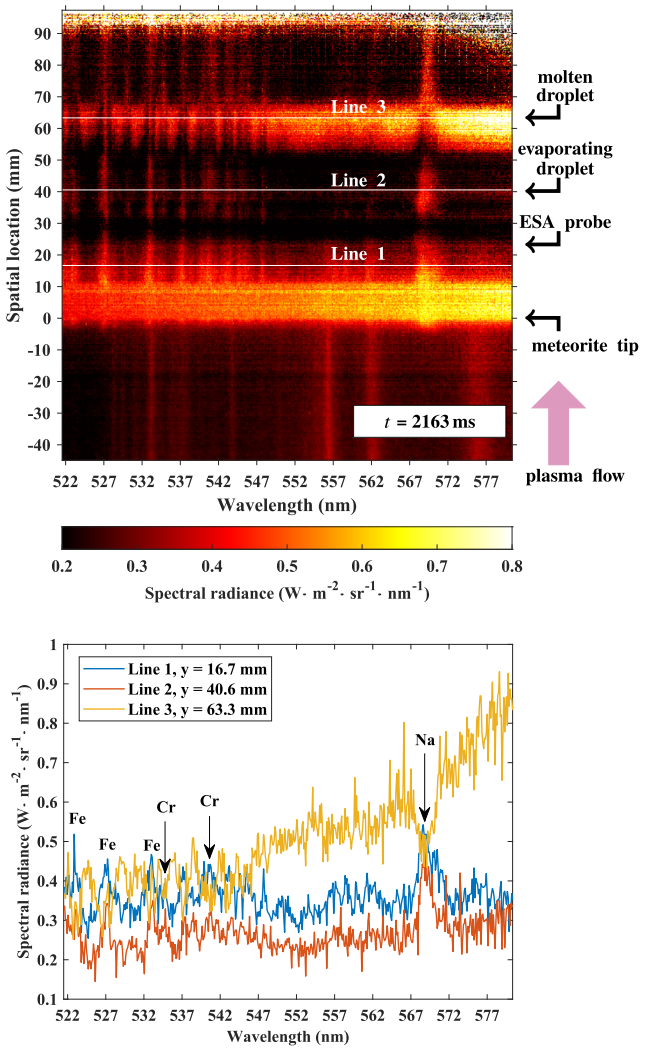

FIG. 4. Calibrated spectral image (shown in false color) of an ablating Knyahinya meteorite sample (top) with the wavelength distribution of radiance extracted from discrete spatial locations (bottom).

The calibrated video of the spectral images shows multiple interesting features occurring in a very short time scale when the meteorite sample is exposed to the plasma flow. From the video data, it was also possible to track the spectral evolution of the molten droplets as they travel downstream originating from the meteorite sample. As an example, three frames (5 ms apart) from the same test case are shown in Fig. 5. Clearly visible in Fig. 5 are two molten droplets originating from the meteorite as they move and spectrally evolve, traveling downstream in the flow. Even though the video was recorded at a frame rate of 1 kHz, the frames chosen here are 5 ms

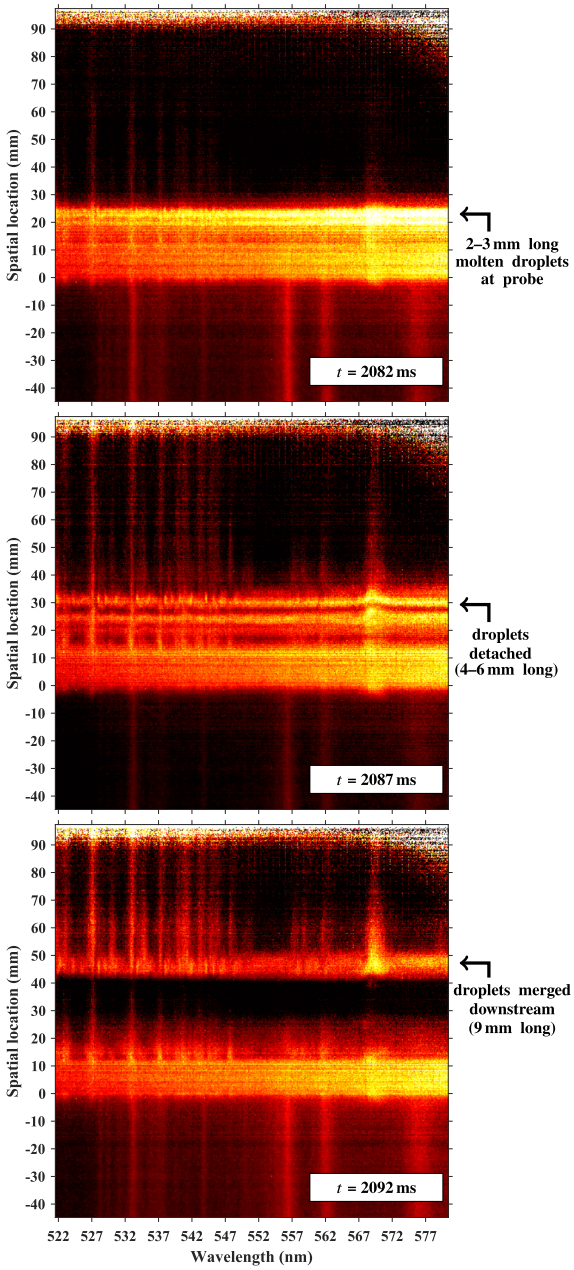

FIG. 5. Tracking of the molten droplets from the Knyahinya meteorite sample and their evolution as they travel downstream; the frames shown are 5 ms apart from each other.

apart to better illustrate the differences. The frame-to-frame tracking of such molten droplets can also be used to calculate the change in their sizes (due to elongation from shear) and to calculate their velocities downstream. The size of the droplets can be an approximation of the typical fragment sizes neglecting the reduction in size due to melting and vaporization on the surface. The change in sizes of the droplets is indicated in Fig. 5, which shows that the droplets elongate as they travel downstream coupled with evaporation. Even though the change in sizes can be observed with ordinary high-speed video recording, this new instrument is advantageous as it simultaneously shows the spectral and spatial evolution of droplets.

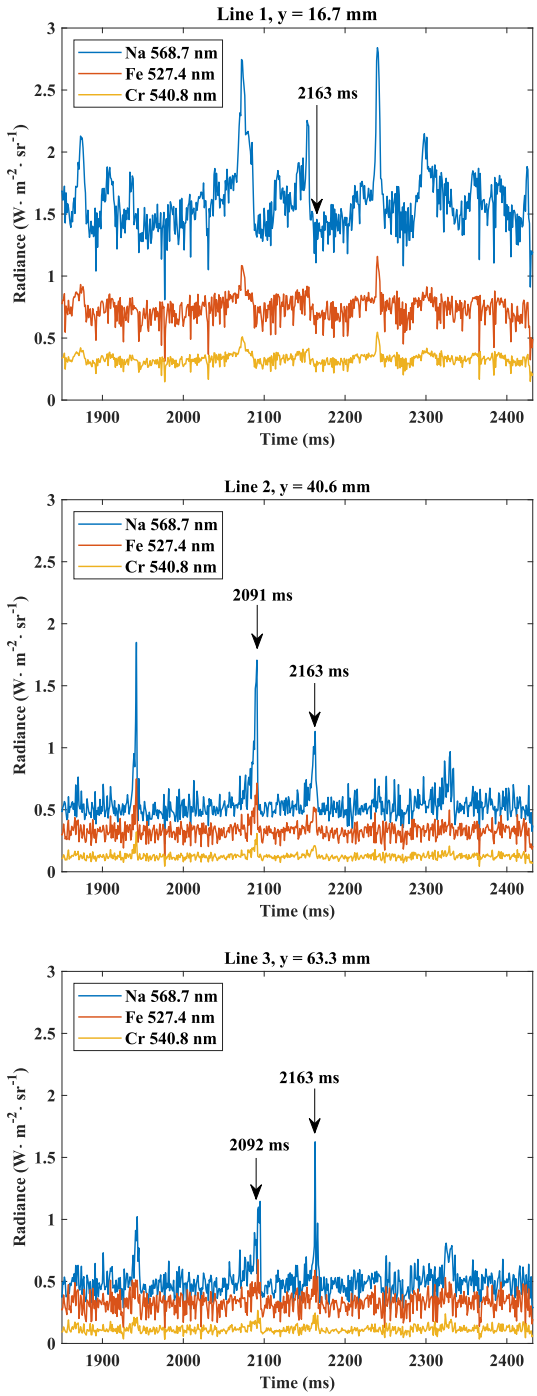

FIG. 6. Temporal evolution of emission intensity of selected atomic lines at various spatial locations.

The investigation on the change in emission intensity and rise/decay of species between frames and at various spatial locations can also be performed with this high frame rate recording of the emission spectra. The spatial locations shown in Fig. 4 (lines 1, 2, and 3) were temporally tracked each frame (every 1 ms) for some selected atomic emission lines: Na (568.7 nm), Fe (527.4 nm), and Cr (540.8 nm). The selected atomic lines were spectrally integrated at a given spatial location from each frame, and the temporal evolution of the resulting radiance of each species is plotted in Fig. 6. From Fig. 6, it is possible to observe the rise/decay of the species emission with respect to time. A clear drop in the emission intensity was observed at locations downstream. The peaks of radiance can be inferred as a presence of the meteorite fragments/droplets crossing that spatial location at those time instances. Some of the intense peaks, for example, those of Na, show disproportionate drop in radiance downstream indicating different levels of evaporation or that the fragment has moved out of the plane of sight. The time instant (t = 2163 ms) corresponding to the frame in Fig. 4 is also annotated in Fig. 6 showing peaks of radiance indicating the crossover of bright droplets at that location. Similar analyses could be carried out for other species and locations, as enabled by the high frame rate recording of spectral images with simultaneous spatial resolution.

VI. CONCLUSIONS

The application of high frame rate emission spectroscopy is demonstrated in this work, as applied to the meteorite ablation experiments in the high enthalpy plasma wind tunnel facility PWK1. The results obtained at 1 kHz frame rate proved to be very useful in studying the ablation of meteorite in detail including the meteorite melting into droplets and flowing away downstream and the spatial distribution of spectral emissions arising from the meteorite fragments. The faint iron lines can be analyzed with this new setup, allowing for a detailed time and spatial resolution during a transient ablation process. This novel setup has potential applications in many such high-speed phenomena, particularly the ablation of thermal protection materials and breakup during re-entry testing in high enthalpy ground test facilities.

ACKNOWLEDGMENTS

Financial support for this project from ESA Contract No. 4000128930/19/NL/SC, the Slovak Research and Development Agency Grant No. APVV-16-0148, and the Slovak Grant Agency for Science Grant No. VEGA-01/0596/18 is gratefully acknowledged. The authors would like to thank the members of HEFDiG for support in the experiments and discussions. The assistance from the technicians at IRS and NHMV workshops is greatly appreciated.

DATA AVAILABILITY

The data that support the findings of this study are available from the corresponding author upon reasonable request.

REFERENCES

[1]B. Cruden, R. Martinez, J. H. Grinstead, and J. Olejniczak, "Simultaneous vacuum ultraviolet through near IR absolute radiation measurement with spatiotemporal resolution in an electric arc shock tube," in *41st Thermophysics Conference* (AIAA, 2009).
[2]T. Hermann, S. Loehle, F. Zander, and S. Fasoulas, "Emission spectroscopic assessment of plasma wind tunnel aerothermodynamics," in *8th Workshop on Radiation of High Temperature Gases* (ESA, 2016).
[3]M. W. Winter, M. Auweter-Kurtz, and C. Park, "Determination of temperatures and particle densities in a subsonic high enthalpy plasma flow from emission spectroscopic measurements," in *32nd AIAA Plasmadynamics and Lasers Conference* (AIAA, 2001).
[4]R. Ravichandran, "Ablation and radiation in hypervelocity earth-entry flows," Ph.D. thesis, The University of Queensland, 2019.
[5]F. Zander, S. Loehle, T. Hermann, and H. Fulge, "Fabry-Perot spectroscopy for kinetic temperature and velocity measurements of a high enthalpy air plasma flow," J. Appl. Phys. D **50**, 335202 (2017).
[6]D. Subasinghe, M. D. Campbell-Brown, and E. Stokan, "Physical characteristics of faint meteors by light curve and high-resolution observations, and the implications for parent bodies," Mon. Not. R. Astron. Soc. **457**, 1289 (2016).
[7]V. Vojáček, J. Borovicka, P. Koten, P. Spurný, and R. Štork, "Catalogue of representative meteor spectra," Astron. Astrophys. **580**, A67 (2015).
[8]P. Matlovič, L. Kornoš, M. Kováčová, J. Tóth, and J. Licandro, "Characterization of the June epsilon Ophiuchids meteoroid stream and the comet 300P/Catalina," Astron. Astrophys. **636**, A122 (2020).
[9]J. Tóth, L. Kornoš, P. Zigo, Š. Gajdoš, D. Kalmančok, J. Világi, J. Šimon, P. Vereš, J. Šilha, M. Buček, A. Galád, P. Rusňák, P. Hrábeck, F. Ďuriš, and R. Rudawska, "All-sky meteor orbit system AMOS and preliminary analysis of three unusual meteor showers," Planet. Space Sci. **118**, 102 (2015).
[10]S. Loehle, F. Zander, T. Hermann, M. Eberhart, A. Meindl, R. Oefele, J. Vaubaillon, F. Colas, P. Vernazza, A. Drouard, and J. Gattacceca, "Experimental simulation of meteorite ablation during Earth entry using a plasma wind tunnel," Astrophys. J. **837**, 112 (2017).
[11]S. Loehle, S. Fasoulas, G. Herdrich, T. Hermann, B. Massuti-Ballester, A. Meindl, A. S. Pagan, and F. Zander, "The plasma wind tunnels at the Institute of Space Systems: Current status and challenges," in *46th Aerodynamic Measurement Technology and Ground Testing Conference* (AIAA, 2016).
[12]M. Auweter-Kurtz, P. Endlich, G. Herdrich, H. Kurtz, T. Laux, S. Loehle, E. Schreiber, T. Wegmann, and M. W. Winter, "Ground testing facilities for TPS qualification at the Institut für Raumfahrt systeme," in *4th European Symposium on Aerothermodynamics for Space Applications* (ESA, 2001), Vol. SP-487, pp. 655–663.
[13]W. Röck, M. Auweter-Kurtz, P. Dabalà, H. Früholz, H. Habiger, and S. Laure, "Experimental simulation of the entry of Huygens into the Titan atmosphere for the thermal protection qualification," in *44th Congress of the International Astronautical Federation, IAF-93-I.3.227* (Graz, Austria, 1993).
[14]D. Leiser, S. Loehle, F. Zander, R. Choudhury, D. Buttsworth, and S. Fasoulas, "Spacecraft material tests under aerothermal and mechanical reentry loads," in *AIAA Scitech 2019 Forum* (AIAA, 2019).
[15]T. Hermann, S. Löhle, F. Zander, and S. Fasoulas, "Measurement of the aerothermodynamic state in a high enthalpy plasma wind-tunnel flow," J. Quant. Spectrosc. Radiat. Transfer **201**, 216–225 (2017).
[16]F. Zander, T. Marynowski, and S. Loehle, "High-speed imaging of high-frequency effects of a CO_2 plasma flow," J. Thermophys. Heat Transfer **31**, 451 (2017).
[17]A. Andrianatos, "Ground testing at superorbital flight conditions in a large scale expansion tube," Ph.D. thesis, The University of Queensland 2020.